Nanoscale Research Letters
a SpringerOpen Journal

NANO EXPRESS Open Access

Large-scale fabrication of boron nitride nanotubes with high purity via solid-state reaction method

An Pan[1] and Yongjun Chen[1,2*]

Abstract

An effective solid-state reaction method is reported for synthesizing boron nitride nanotubes (BNNTs) in large scale and with high purity by annealing amorphous boron powder and ferric chloride ($FeCl_3$) catalyst in ammonia atmosphere at elevated temperatures. $FeCl_3$ that has rarely been utilized before is introduced not only as a catalyst but also as an efficient transforming agent which converts boron powder into boron chloride (BCl_3) vapor in situ. The nanotubes are bamboo in shape and have an average diameter of about 90 nm. The effect of synthetic temperatures on nanotube morphology and yield is investigated. The photoluminescence (PL) measurement shows emission bands of the nanotubes at 354, 423, 467, and 666 nm. A combined growth mechanism of vapor–liquid-solid (VLS) and solid–liquid-solid (SLS) model is proposed for the formation of the BNNTs.

Keywords: Boron nitride nanotubes; Fabrication; Photoluminescence property; Growth mechanism

Background

As an isostructural and isoelectronic analog to carbon nanotubes (CNTs), boron nitride nanotubes (BNNTs) have attracted more and more attention on account of their superb mechanical property [1], outstanding thermal conductivity and stability [2], excellent radiation shielding [3], strong light emissions [4], and hydrogen storage capacity especially the bamboo-shaped BNNTs [5]. In addition, recent theory simulations reveal that metal-doped (e.g., Fe, Al) BNNTs seem to be more sensitive to some specific absorbates [6,7]. BNNTs are not cytotoxic and can be functionalized for interaction with proteins and cells [8]. Partially vertically aligned BNNT films deposited on Si substrate exhibit strong water repellency [9]. All these fascinating properties make BNNTs promising applications in many areas such as lasing action, gas detective sensors, nanocoating for composites, reinforcement additive [10], hydrogen storage devices [11], and biomedical materials.

Since the discovery of BNNTs in 1995 [12], the main approaches known for the growth of CNTs have been modified to synthesize BNNTs as well, for instance, arc discharge [13], laser ablation [14], and chemical vapor deposition [5]. Unfortunately, however, the yield or purity of BNNTs prepared by such methods is normally disappointing in comparison with that of CNTs. The demands of property investigation and applications are required for an effective route to mass production of BNNTs with high purity. Chen et al. [15] developed a ball milling and annealing method as potential for large-scale production of BNNTs, which gave a conception that a solid-state reaction method would be an alternative technique in bulk synthesis of BNNTs. Nonetheless, particles usually coexisted with BNNTs in the product, which needed further purification process before application. In the current study, we report an effective solid-state reaction method which offers BNNTs with both large quantity and high purity by annealing a highly homogenous precursor composed of amorphous boron (B) powder and ferric chloride ($FeCl_3$) in flowing ammonia (NH_3) atmosphere. To the best of our knowledge, $FeCl_3$ has never been employed as the catalyst for the synthesis of BNNTs. Furthermore, $FeCl_3$ could also act as a crucial transforming agent that converted solid-state

* Correspondence: chenyj99@163.com
[1]College of Chemistry & Chemical Engineering, Guangxi University, Nanning 530004, China
[2]Key Lab of Advanced Materials of Tropical Island Resources, Ministry of Education, College of Materials and Chemical Engineering, Hainan University, Haikou 570228, China

B powders to gaseous boron chloride (BCl_3) in situ. The gaseous BCl_3 possessed high reaction activity and guaranteed the formation of BNNTs under NH_3 flow. The effect of synthetic temperature on the morphology and the growth mechanism of the BNNTs was discussed in detail. The photoluminescence (PL) property of the synthesized BNNTs was also investigated.

Methods

Synthesis of BNNTs

In a typical procedure, amorphous B powders and $FeCl_3 \cdot 6H_2O$ with a molar ratio of 1:0.05 were selected as the raw materials. Firstly, $FeCl_3 \cdot 6H_2O$ was dissolved in absolute ethyl alcohol, then B powders were added into the solution. The mixture was stirred and heated in the water bath at 40°C for 2 h in order to evaporate the solvent. Then the obtained paste-like mixture was dried at 55°C to thoroughly remove the ethanol. After, a highly homogeneous distributed precursor was prepared. The precursor was loaded into an alumina boat which was placed at the center of a tube furnace. Before heating up, high-purity NH_3 flow was introduced to flush out the residual air in the chamber. Then the furnace was heated to 1,200°C at 50 mL min^{-1} NH_3 flow and maintained for 5 h. Finally, the furnace was naturally cooled to ambient temperature under the protection of N_2 flow.

Characterization of BNNTs

Afterwards, it was found that the color of the upper layered staring materials changed from brown into white; the white product was characterized to be BN nanosheet self-assembled microwires and will be discussed elsewhere. Beneath the white product, a gray product was obtained in the boat. The gray product was collected and characterized by scanning electron microscopy (SEM, Zeiss Merlin; Carl Zeiss AG, Oberkochen, Germany), transmission electron microscopy (TEM) and high-resolution TEM (HRTEM, JEOL JEM-2011; JEOL Ltd., Tokyo, Japan) equipped with X-ray energy dispersive spectrometer (EDS), and electron energy loss spectroscopy (EELS, FEI Titan 80–300; FEI, Hillsboro, OR, USA). The PL property of the product was measured at room temperature (Edinburgh FLS920, 300-nm excitation; Edinburgh Instruments, Hertfordshire, UK).

Results and discussion

The SEM images of the as-synthesized sample are shown in Figure 1. Low-magnification image (Figure 1a) exhibits that a large quantity of one-dimensional (1D) nanostructures is synthesized. The nanostructures are dense and relatively pure (no obvious particles can be observed). Figure 1b shows the high-magnification image of the nanostructures. It reveals clearly that the nanostructures are bamboo in shape (i.e., nanotubes) with smooth surfaces. The diameters of the nanotubes vary from 20 nm to more than 100 nm with a mean value of about 90 nm. Further magnified image (the inset) shows a particle attached at the end of a nanotube, which is normally regarded as a typical symbol of vapor–liquid-solid (VLS) growth model.

The TEM image shown in Figure 2a illustrates more clearly that the nanostructure is a bamboo-shaped nanotube composed of a series of hermetical compartments that are tightly connect together. At the same time, catalyst particles are observed within the cavity of the nanotube, which is consistent with the SEM observation. Figure 2b demonstrates the HRTEM image of a joint connecting the wall and the compartment of the nanotube. The lattice fringes of the wall and compartment can be clearly seen with interlayer spacings of approximately 0.336 and 0.335 nm, respectively, which correspond to (002) planes of hexagonal BN (h-BN) crystals. The slight difference of interlayer spacings between the wall and compartment can be attributed to the measurement error. Figure 2c is the EDS spectrum taken from the nanotube walls, demonstrating major peaks of B, N, and Cu with small amounts of O, Fe, and Cr. The Cu peaks should come from the copper TEM grid, while O peak is ascribed to the slight surface oxidation or oxygen adsorption of the nanotube in air. The weak Fe peaks should be caused by the inclusion of $FeCl_3$. We speculate that Cr signal may come from the impurities in the raw materials. Therefore,

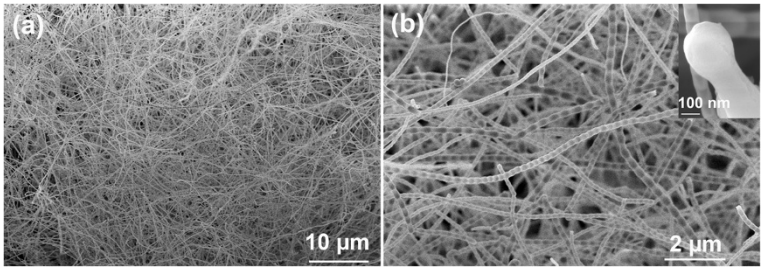

Figure 1 SEM images of the product synthesized at 1,200°C. (a) Low-magnification image. **(b)** High-magnification images. The inset shows a particle attached at the end of a nanotube.

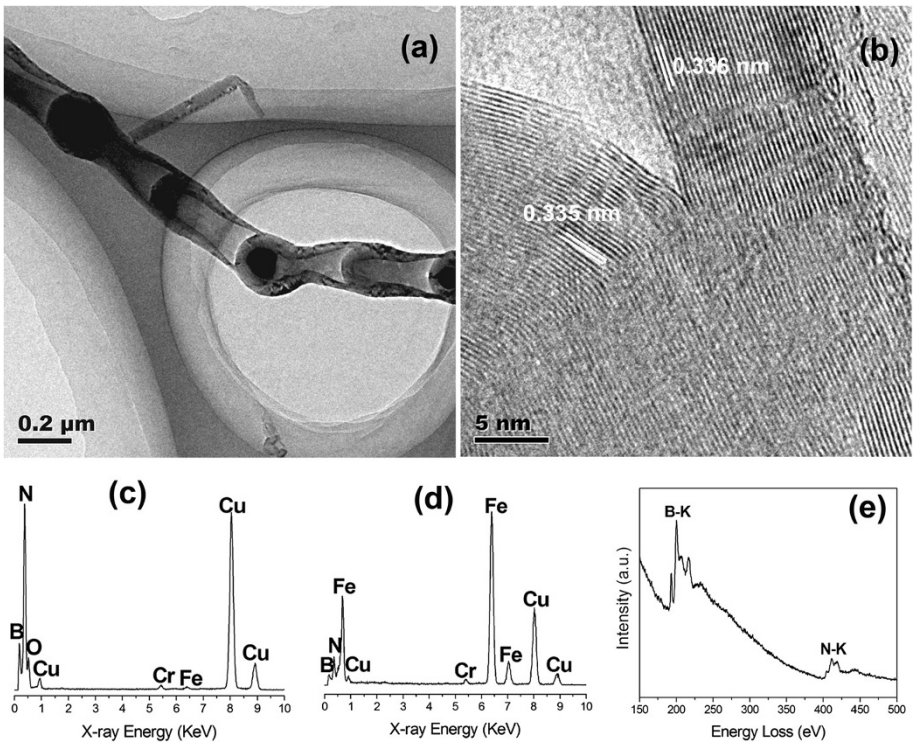

Figure 2 TEM images and composition of the synthesized BNNTs. (a) TEM image. **(b)** HRTEM image. **(c)** EDS result of the nanotube walls. **(d)** EDS result of the encapsulated particles within the nanotube. **(e)** EELS spectrum of the nanotube.

it can be roughly concluded that the nanotube is composed of BN. Figure 2d shows the EDS result of an encapsulated particle. Dominating peaks of B, N, Fe, and Cu along with a low level of Cr are detected. Apparently, the intensity of Fe signal increases dramatically. It is therefore believed that Fe-containing alloy droplets exist historically during the growth of BNNTs. The chemical composition of the nanotube is further determined by means of EELS. Figure 2e depicts a typical EELS spectrum that has two pronounced adsorption peaks of B and N characteristic K-edges at 188 and 401 eV, respectively. For each K-edge adsorption, a discernible π^* peak accompanied by a broad σ^* peak can be observed, which is a representative feature of an sp^2-hybridized state. Hence, it is confirmed that the synthesized product comprised bamboo-shaped BNNTs.

Figure 3 shows the PL property of the BNNTs. Four main emission bands centered at 354, 423, 467, and 666 nm are observed. Normally, the possibility of a material to demonstrate luminescence relies on the intrinsic band edge structure and other internal or external factors (intrinsic/extrinsic defects) [16,17]. Some PL emission peaks in the range 300 to 400 nm have been reported [18-21] that originate from residual impurities such as carbon and oxygen [22] rather than interband transitions. Therefore, the band at about 354 nm in our study could be assigned to the impurity centers (possibly attributed to oxygen impurities, as is supported by the EDS result). The emission bands located at 423 and 467 nm could be attributed to the intrinsic emission from bamboo-shaped BNNTs, which possess a great deal of bent layers and associated defects similar to the cup-shaped BN layers in the bamboo-shaped nanotubes [4]. There have been no correlated reports on the PL band

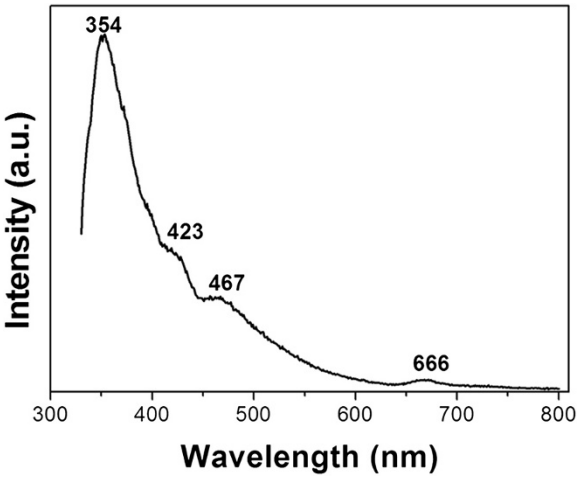

Figure 3 Photoluminescence property of the synthesized BNNTs.

located at 666 nm for h-BN. However, Zhu et al. stated that the emission band at 700 nm of BN whiskers might originate from defect-trapped states (vacancy-type defect) and a quantum confinement effect [23]. Long-wavelength PL emissions at 728 and 703 nm were reported by our group in BN nanowires [24] and nanotubes [25] due to the intrinsic lattice defects as well. Chen et al. [4] interpreted 680-nm PL emissions in periodic yard-glass-shaped BNNTs to be ascribed to the lattice defects in the periodical structures and their inserting connection mode. Therefore, it is reasonable that intrinsic lattice defects are responsible for the emission band at 666 nm in the current study.

Figure 4a,b shows the SEM images of the product synthesized at 1,150 and 1,250°C, respectively. No nanotubes can be observed in the case of 1,150°C (Figure 4a). When the temperature increases to 1,250°C, the yield of BNNTs decreases obviously and considerable amounts of particles are formed in the product (Figure 4b). Moreover, careful observation from the enlarged image (the inset) reveals that the nanotubes are generally in the form of a quasi-cylindrical structure.

Based on the results described above, the growth process of the BNNTs is illustrated as follows:

$$6FeCl_3\ (s) + 2NH_3 \rightarrow 6FeCl_2 + (g) + N_2\ (g)$$
$$\Delta G < 0 \text{ (temperature in range of } 0\sim1250^{\circ}C) \quad (1)$$

$$FeCl_2(s) \rightarrow FeCl_2(l) \quad (2)$$

$$FeCl_2(l) \rightarrow FeCl_2(g)$$
$$\Delta G\ (1150\sim1250^{\circ}C) = -14.820 \sim -24.670\ \text{kJ} \quad (3)$$

$$3FeCl_2(g) + 2B\ (s) \rightarrow 2BCl_3(g) + 3Fe\ (l)$$
$$\Delta G\ (1150\sim1250^{\circ}C) = -44.265 \sim -22.991\ \text{kJ} \quad (4)$$

$$3FeCl_2(l) + 2B\ (s) \rightarrow 2BCl_3(g) + 3Fe\ (l)$$
$$\Delta G\ (1150\sim1250^{\circ}C) = -88.726 \sim -97.000\ \text{kJ} \quad (5)$$

$$BCl_3(g) + NH_3(g) \rightarrow BN\ (s) + 3HCl\ (g)$$
$$\Delta G\ (1150\sim1250^{\circ}C) = -216.077 \sim -226.045\ \text{kJ} \quad (6)$$

At first, $FeCl_3$ is reduced to $FeCl_2$ by NH_3. Along with heating up, $FeCl_2$ goes through a series of transformation from solid phase to liquid and gas phase (Equations 1, 2, and 3). Proved by the thermodynamic calculations, $FeCl_2$ boils up mildly, and liquid-phase $FeCl_2$ is more reactive than gas-phase $FeCl_2$ in transforming solid B powders into BCl_3 vapor at experimental temperatures (Equations 4 to 5). When the temperature reaches to 1150 to 1,250°C, Fe melts down partially and absorbs the surrounding vapors of BCl_3 and NH_3 to form Fe-B-N alloy droplets. When the concentrations of the BN species in the droplets are greater than the saturation threshold, BN shells begin to precipitate layer by layer around the droplets (Equation 6). The thickness of BN shell gradually increases, and the diameter of newly formed BN shell decreases with the inward growth of the BN shells. The increasing curvature caused by smaller diameter of the inner BN shell results in growing stress energy between the shells and the catalyst core [26]. When the stress energy reaches a certain degree, the molten core will be expulsed from the defective region of the BN shells and sequentially shrinks to locate at the door of the torn elongated BN shell. The expulsed catalyst core keeps on absorbing gas species and the next growth proceeds via the same way. The whole process is extremely similar to the VLS growth of bamboo-shaped BNNTs reported in literatures [27,28]. Particularly worth mentioning in the current study is that the catalyst core will be expulsed out wholly or partially depending on the value of stress energy, which can explain the TEM observation of discontinuous encapsulated particles within the compartment cavities of the nanotubes. As the described procedure occurs in cycles, bamboo-shaped structures are finally formed. It can be found that the growth process of the nanotubes not only involves the absorption and dissolution of NH_3 and BCl_3 from gas phase but also includes the relatively slow diffusion of B from solid phase to the alloy droplets, which

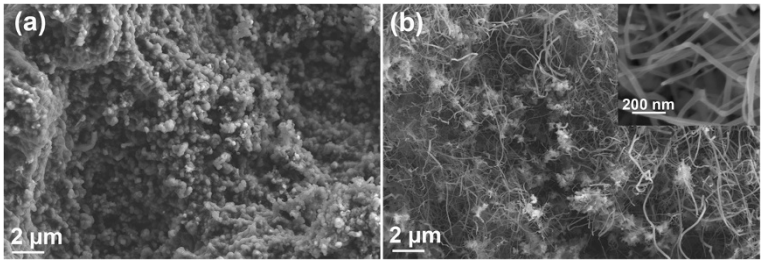

Figure 4 SEM images of the products synthesized at different temperatures. (a) 1,150°C. **(b)** 1,250°C.

may determine the final growth rate of the nanotubes. Therefore, the growth of BNNTs in the current study follows a combination mechanism of VLS and solid–liquid-solid (SLS) models [27,29].

When the temperature lowers to 1,150°C, the reactions (Equations 4 and 5) could still be carried out but the reaction rates reduce significantly. Moreover, the diffusion rate of B/N atoms on alloy droplet surfaces also decreases. Thus, the insufficiency of BCl_3 vapor results in the formation of particles rather than nanotubes. As the reaction temperature rises to 1,250°C, both the diffusion rates of B/N atoms through the surface and the bulk of the catalyst droplets increase. However, the surface diffusion rate enhances significantly [30], which favors the formation of nanotube walls rather than the compartment layers. In addition, the crystalline perfection of the nanotubes improves with the rise of temperature and the compartment will endure stronger stress. Hence, a quasi-cylindrical structure with less strain will be more favorable based on the principle of minimum free energy. However, the nitridation reaction (Equation 6) performs very fast and the concentration of BCl_3 vapor within the chamber increases so quickly within a short period of time that some of them will be flushed out of the chamber by NH_3 flow. Therefore, the yield of the BNNTs diminishes.

Conclusions

High-purity BNNTs are successfully synthesized in large quantity by annealing $FeCl_3$ and amorphous boron in NH_3 atmosphere. $FeCl_3$ not only provides catalyst Fe but also reacts with boron powders to generate BCl_3 vapor in situ, which is vital for the formation of BNNTs. The BNNTs are bamboo in shape with an average diameter of about 90 nm. A combination growth mechanism of VLS and SLS models is proposed to govern the formation of BNNTs. The synthetic temperature affects the morphology and yield of the BNNTs greatly through influencing the generation of BCl_3 vapor. With the rise of temperature, the structure of the BNNTs has a tendency to form from bamboo toward cylindrical, but the yield of the BNNTs tends to be lower. The BNNTs exhibit strong PL emissions at 354 nm, suggesting their potential applications in optical and electronic devices.

Competing interests

The authors declare that they have no competing interests.

Authors' contributions

AP performed the syntheses and characterization. YC was in charge of designing and supervision of the experiments. Both authors read and approved the final manuscript.

Acknowledgements

The project is supported by the National Science Foundation of China (Grant Nos. 51162001 and 51362008), Hainan University Scientific Research Funding (Grant No. kyqd1240), and local service project (Grant No. HDSF201308). The work makes use of the resources of the Beijing National Center for Electron Microscopy.

Received: 1 August 2014 Accepted: 23 September 2014
Published: 7 October 2014

References

1. Golberg D, Bando Y, Tang C, Zhi C: **Boron nitride nanotubes.** *Adv Mater* 2007, **19:**2413–2432.
2. Chang CW, Fennimore AM, Afanasierv A, Okawa D, Ikuno T, Garcia H, Li D, Majumdar A, Zettl A: **Isotope effect on the thermal conductivity of boron nitride nanotubes.** *Phys Rev Lett* 2006, **97:**085901.
3. Yu J, Chen Y, Elliman RG, Petravic M: **Isotopically enriched ^{10}BN nanotubes.** *Adv Mater* 2006, **18:**2157–2160.
4. Chen ZG, Zou J, Liu G, Li F, Cheng HM, Sekiguchi T, Gu M, Yao XD, Wang LZ, Lu GQ: **Long wavelength emissions of periodic yard-glass shaped boron nitride nanotubes.** *Appl Phys Lett* 2009, **94:**023105.
5. Tang C, Bando Y, Ding X, Qi S, Golberg D: **Catalyzed collapse and enhanced hydrogen storage of BN nanotubes.** *J Am Chem Soc* 2002, **124:**14550–14551.
6. Zhang YQ, Liu YJ, Liu YL, Zhao JX: **Boosting sensitivity of boron nitride nanotube (BNNT) to nitrogen dioxide by Fe encapsulation.** *J Mol Graph Model* 2014, **51:**1–6.
7. Azizi K, Salabat K, Seif A: **Methane storage on aluminum-doped single wall BNNTs.** *Appl Surf Sci* 2014, **309:**54–61.
8. Chen X, Wu P, Rousseas M, Okawa D, Gartner Z, Zettl A, Bertozzi CR: **Boron nitride nanotubes are noncytotoxic and can be functionalized for interaction with protein and cells.** *J Am Chem Soc* 2009, **131:**890–891.
9. Lee CH, Drelich J, Yap YK: **Superhydrophobicity of boron nitride nanotubes grown on silicon substrates.** *Langmuir* 2009, **25:**4853–4860.
10. Tatarko P, Grasso S, Porwal H, Chlup Z, Saggar R, Dlouhy I, Reece MJ: **Boron nitride nanotubes as a reinforcement for brittle matrices.** *J Europ Ceram Soc* 2014. http://dx.doi.org/10.1016/j.jeurceramsoc.2014.03.028.
11. Terao T, Bando Y, Mitome M, Kurashima K, Zhi CY, Tang CC, Golberg D: **Effective synthesis of surface-modified boron nitride nanotubes and related nanostructures and their hydrogen uptake.** *Phys E* 2008, **40:**2551–2555.
12. Chopra NG, Luyken RJ, Cherrey K, Crespi VH, Cohen ML, Louie SG, Zettl A: **Boron nitride nanotubes.** *Science* 1995, **269:**966–967.
13. Loiseau A, Willaime F, Demoncy N, Hug G, Pascard H: **Boron nitride nanotubes with reduced numbers of layers synthesized by arc discharge.** *Phys Rev Lett* 1996, **76:**4737–4740.
14. Golberg D, Bando Y, Eremets M, Takemura K, Kurashima K, Yusa H: **Nanotubes in boron nitride laser heated at high pressure.** *Appl Phys Lett* 1996, **69:**2045–2047.
15. Chen Y, Fitz Gerald J, Williams JS, Bulcock S: **Synthesis of boron nitride nanotubes at low temperatures using reactive ball milling.** *Chem Phys Lett* 1999, **299:**260–264.
16. Gupta BK, Shanker V, Arora M, Haranath D: **Photoluminescence and electron paramagnetic resonance studies of springlike carbon nanofibers.** *Appl Phys Lett* 2009, **95:**073115.
17. Jaffrennou P, Barjon J, Lauret JS, Maguer A, Golberg D, Attal-Tretout B, Ducastelle F, Loiseau A: **Optical properties of multiwall boron nitride nanotubes.** *Phys Stat Sol B* 2007, **244:**4147–4151.
18. Yu J, Yu D, Chen Y, Chen H, Lin MY, Cheng BM, Li J, Duan W: **Narrowed bandgaps and stronger excitonic effects from small boron nitride nanotubes.** *Chem Phys Lett* 2009, **476:**240–243.
19. Su CY, Juang ZY, Chen KF, Cheng BM, Chen FR, Leou KC, Tsai CH: **Selective growth of boron nitride nanotubes by plasma-assisted and iron-catalytic CVD methods.** *J Phys Chem C* 2009, **113:**14681–14688.
20. Jaffrennou P, Barjon J, Schmid T, Museur L, Kaneav A, Lauret JS, Zhi CY, Tang C, Bando Y, Golberg D, Attal-Tretout B, Ducastelle F, Loiseau A: **Near-band-edge recombinations in multiwalled boron nitride nanotubes: cathodoluminescence and photoluminescence spectroscopy measurements.** *Phys Rev B* 2008, **77:**235422.
21. Su CY, Chu WY, Juang ZY, Chen KF, Cheng BM, Chen FR, Leou KC, Tsai CH: **Large-scale synthesis of boron nitride nanotubes with iron-supported catalysts.** *J Phys Chem C* 2009, **113:**14732–14738.
22. Taniguchi T, Watanabe K: **Synthesis of high-purity boron nitride single crystals under high pressure by using Ba-BN solvent.** *J Cryst Growth* 2007, **303:**525–529.

23. Zhu CY, Bando Y, Xue DF, Sekiguchi T, Golberg D, Xu FF, Liu QL: **New boron nitride whiskers: showing strong ultraviolet and visible light luminescence.** *J Phys Chem B* 2004, **108:**6193–6196.
24. Chen YJ, Chi B, Mahon DC, Chen Y: **An effective approach to grow boron nitride nanowires directly on stainless-steel substrates.** *Nanotechnology* 2006, **17:**2942–2946.
25. Li J, Li JB, Yin YC, Chen YJ, Bi XF: **Water-assisted chemical vapor deposition synthesis of boron nitride nanotubes and their photoluminescence property.** *Nanotechnology* 2013, **24:**365605.
26. Zhang XX, Li ZQ, Wen GH, Fung KK, Chen JL, Li YD: **Microstructure and growth of bamboo-shaped carbon nanotubes.** *Chem Phys Lett* 2001, **333:**509–514.
27. Bi XF, Yin YC, Li JB, Chen YJ, Li J, Su QQ: **A co-precipitation and annealing route to the large-quantity synthesis of boron nitride nanotubes.** *Solid State Sci* 2013, **25:**39–44.
28. Huo KF, Hu Z, Fu JJ, Xu H, Wang XZ, Chen Y: **Microstructure and growth model of periodic spindle-unit BN nanotubes by nitriding Fe-B nanoparticles with nitrogen/ammonia mixture.** *J Phys Chem B* 2003, **107:**11316–11320.
29. Mo LB, Chen YJ, Luo LJ: **Solid-state reaction synthesis of boron carbonitride nanotubes.** *Appl Phys A-Mater Sci Process* 2010, **100:**129–134.
30. Kim NS, Lee YT, Park J, Ryu H, Lee HJ, Choi SY, Choo J: **Dependence of the vertically aligned growth of carbon nanotubes on the catalysts.** *J Phys Chem B* 2002, **106:**9286–9290.

doi:10.1186/1556-276X-9-555
Cite this article as: Pan and Chen: Large-scale fabrication of boron nitride nanotubes with high purity via solid-state reaction method. *Nanoscale Research Letters* 2014 **9**:555.